REVIEW ARTICLE
https://doi.org/10.1038/s41928-018-0173-2

nature electronics

Terahertz integrated electronic and hybrid electronic–photonic systems

Kaushik Sengupta[1*], Tadao Nagatsuma[2] and Daniel M. Mittleman[3]

The field of terahertz integrated technology has undergone significant development in the past ten years. This has included work on different substrate technologies such as III–V semiconductors and silicon, work on field-effect transistor devices and heterojunction bipolar devices, and work on both fully electronic and hybrid electronic–photonic systems. While approaches in electronic and photonics can often seem distinct, techniques have blended in the terahertz frequency range and many emerging systems can be classified as photonics-inspired or hybrid. Here, we review the development of terahertz integrated electronic and hybrid electronic–photonic systems, examining, in particular, advances that deliver important functionalities for applications in communication, sensing and imaging. Many of the advances in integrated systems have emerged, not from improvements in single devices, but rather from new architectures that are multifunctional and reconfigurable and break the trade-offs of classical approaches to electronic system design. We thus focus on these approaches to capture the diversity of techniques and methodologies in the field.

The frequency range of 0.1–3.0 THz, which is sandwiched between microwave frequencies at the lower end and optical frequencies at the higher end, has, in the past, been referred to as the terahertz (THz) gap. This was primarily due to lack of efficient methods for generating or detecting signals in this frequency range[1–9]. Over the past few decades, THz systems research has taken a major step forward with the development of laser-based technologies for the generation and detection of THz signals. In these systems, femtosecond lasers combined with ultrafast lightwave-to-THz converters, such as photoconductive antennas and nonlinear optical crystals, are used for both the emitter (transmitter) and detector (receiver). The emergence of this optics-based approach in the late 1980s dramatically lowered the bar for THz measurements for many researchers. Yet, compared with integrated circuits, these optical systems are bulky and expensive. Thus, while promising a wide range of applications in sensing, imaging and communication[8–16], the THz spectrum has not yet delivered on such potential due to a lack of low-cost, portable, efficient technologies.

In the past decade, there has been a significant surge of progress in enabling integrated, compact and efficient chip-scale THz technology, which could close the THz gap in meaningful ways. This progress is a result of a concerted effort stretching across a wide range of areas including solid-state and photonic devices[17–21], two-dimensional (2D) materials[22,23], heterogeneous integration[24] and packaging and system demonstrations[16,25,26]. Considerable work has been directed towards miniaturized THz technology demonstrated with quantum-cascade lasers[27–29], microbolometers[30,31], nanowires[32], novel plasmonic nanostructures[33], metamaterials[34] and ultrafast photoconductive semiconductor materials[35,36]. Importantly, much of the recent effort has been dedicated to exploiting techniques compatible with (or realized in) solid-state semiconductor technology (III–V and silicon based) that can operate at room temperature and can be manufactured at a low cost, exploiting economies of scale. This is a critical departure from the focus on the search for the 'perfect' THz device, and towards a more holistic approach for realizing new system-level properties that can enable a moderately efficient system, which is versatile and programmable. Programmability could include electronic reconfigurability of the wavefront and polarization of the emitted THz fields, for applications in communication, radar and imaging, or dynamic spectral control of the radiated fields for spectroscopy and hyperspectral imaging (Fig. 1). Such versatility is often required for advanced applications, and is generally lacking in many current non-integrated THz platforms.

If history is a guide, then the field of radiofrequency (RF) integrated circuits and systems provides a powerful lesson. Modern-day wireless infrastructure relies on the incredible complexity and reconfigurability of current RF integrated circuits, which would not have been possible without the level of integration supported by silicon integrated circuit technology. The field of THz technology is beginning to experience a similar revolution. Indeed, based on the advances in the field over the past decade, it can be argued that THz electronics is at an inflection point and the field is moving from bridging the THz gap to bridging the 'technology' and 'application' gap.

Owing to its unique position in the spectrum, researchers across electronics and photonics have converged to address the technological challenges in the field. One result of this effort is how various technologies for THz generation have progressed over the past decade in their ability to generate signals in this range (Fig. 1b)[37–64]. Although power is by no means the only important criterion, it is a useful metric for illustrating recent progress.

On the electronics front, III–V-based semiconductor technologies such as InP heterojunction bipolar transistors (HBTs), high electron mobility transistors (HEMTs) and GaAs-based Schottky diodes are now capable of generating power levels at room temperature in the 100 μW–mW range[39,40,43], almost two to five times higher than a decade ago, particularly at frequencies beyond 1 THz. Silicon-based integrated technology, providing a platform for massive integration, has demonstrated complex phased array, imaging and communication systems with output power reaching up to the 100 μW range at 1 THz (ref. [61]). Photonic methods of THz generation have evolved as well, reaching tens of μW of continuous-wave

[1]Department of Electrical Engineering, Princeton University, Princeton, NJ, USA. [2]Graduate School of Engineering Science, Osaka University, Osaka, Japan. [3]School of Engineering, Brown University, Providence, RI, USA. *e-mail: kaushiks@princeton.edu

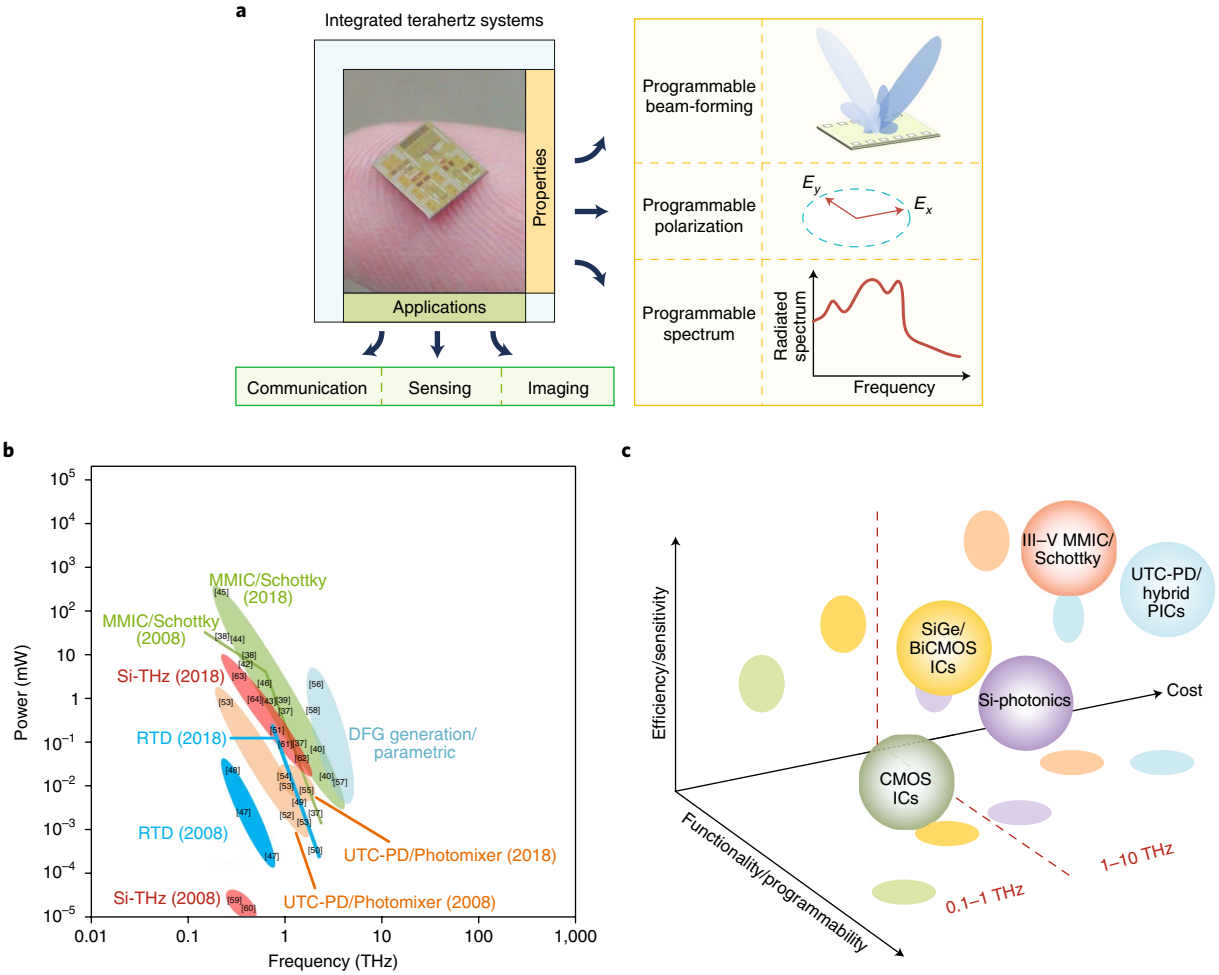

Fig. 1 | Integrated THz systems and the technology landscape. a, Moving the focus from a device-centric approach to enabling complex THz systems that might have moderate efficiency but that are versatile and programmable. This includes properties such as the ability to synthesize or sense THz fields in a reconfigurable manner across spectrum and spatial distribution. Such systems that can be manufactured at low cost and operate at room temperature can be an extremely powerful tool to significantly advance the application space, particularly in imaging and sensing where single modality is often not sufficient. **b**, Progress of THz sources in the past decade showing how a selected set of integrated THz technology has evolved over the past ten years in its ability to generate continuous-wave THz signals at room temperature. The panel is adapted from ref. [2], Springer Nature Ltd, which designated the state-of-the-art technology in 2007. MMIC, microwave monolithic integrated circuits; RTD, resonant tunnel diodes; DFG, difference frequency generation. Numbers in square brackets are reference citations. **c**, While some technologies are better placed than others purely from a signal-generation perspective, there are other considerations that go behind evaluating the optimal THz technology. This includes efficiency, ability to reconfigure the spectrum and field distribution, cost and scalability. A qualitative illustration of technologies in this multidimensional space is captured in the figure. ICs, integrated circuits; UTC-PD, uni-travelling-carrier photodiode; PICs, photonic integrated circuits.

power with photomixer-based approaches[54,55] and mW power level in the 1–2 THz range with difference frequency generation or parametric generation using nonlinear materials[56–58].

While plots of this nature are often used to show the existence (or absence) of technology solutions in the THz range, the requirements for practical THz systems are much more complex, ranging from signal generation (and its efficiency) and detection (and its sensitivity) to fast programmability. The specific issues include beam and frequency reconfiguration, integrability, scalability, size, form factor and cost. A qualitative representation of this complexity, along a few of the relevant axes, is shown in Fig. 1c. Ultimately, the choice of a solid-state technology for a given application and frequency range has to take into consideration all these metrics, across various levels, from device to system.

In this Review Article, we highlight what we consider to be the key innovations that have enabled significant advances in the field of integrated or system-level THz technology. Distinct from other review articles on THz science[8,9], we focus on developments in integrated technology across electronics and photonics, and emphasize the need for convergence between them to develop dependable and deployable THz systems for future applications. In particular, we focus on integrated systems, and the need for reconfigurability, adaptability and scalability, beyond the classical metrics of sensitivity and efficiency.

Electronic approach

In recent years, there have been many advances in device fabrication technology for integrated circuits functioning in the THz range, including both silicon and III–V substrates. When judged solely by transistor-level metrics, InP-based HEMTs and HBTs exhibit superior high-frequency performance when compared with any silicon-based device[18–20]. One metric that can be used to compare various technologies is the cut-off frequency f_{max}. As shown in Fig. 2a, the ability of an active device to absorb power from a source (port-1),

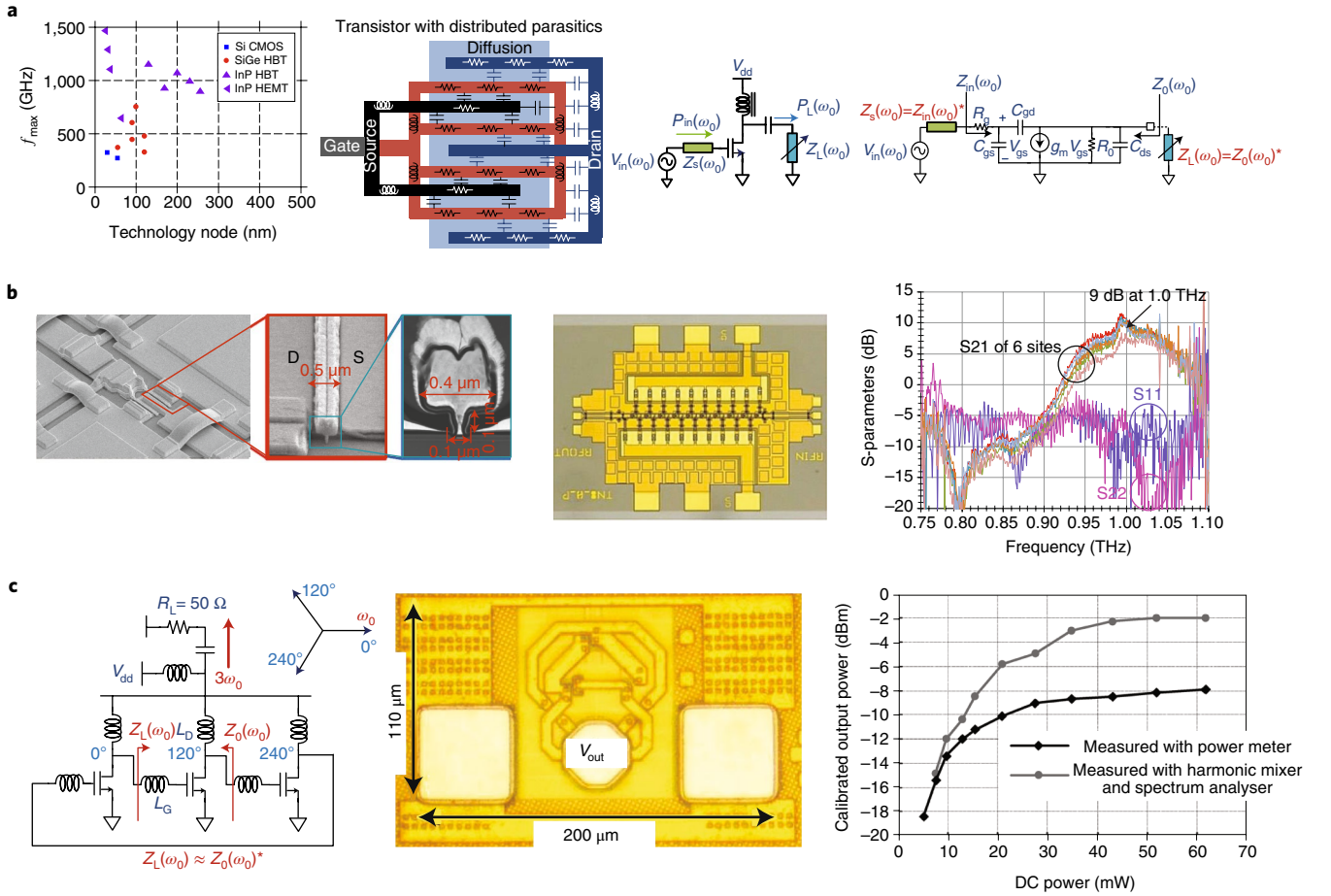

Fig. 2 | High-frequency limits of solid-state devices and THz signal generation. a, The cut-off frequency (f_{max}) of a single device is the frequency at which the optimal power gain falls to unity. f_{max} of InP HEMT transistors have crossed 1.5 THz, while commercially available silicon THz nodes have crossed 0.5 THz. In the figure, $P_{in}(\omega_0)$ ($P_L(\omega_0)$), $V_{in}(\omega_0)$ ($V_L(\omega_0)$) and $Z_{in}(\omega_0)$ ($Z_0(\omega_0)$) represent the input (output) power, voltage and impedance, respectively. These parameters are related through the small-signal operation of the transistor as depicted in the figure. **b**, The first solid-state amplifier above 1 THz with InP-based HEMTs with f_{max} of 1.5 THz (ref. [66]). **c**, Fully integrated oscillators operating close to f_{max} and allowing optimal harmonic power generation beyond f_{max} in the THz range. The example shows 150 μW of power generation at 0.48 THz with the third harmonic of the fundamental signal in a CMOS technology with f_{max} of ~0.17 THz (ref. [81]). Panels adapted from: **b**, ref. [66], IEEE; **c**, ref. [81], IEEE.

amplify it and deliver it efficiently to a second terminal (port-2) depends on the impedances at the two ports at the frequency of interest. The frequency f_{max} represents the frequency at which the unilateral power gain of the device falls to unity[65]. This is an important metric because it fundamentally defines the maximum frequency at which the device can provide power amplification or establish an oscillatory behaviour. The typical method for frequency synthesis at RF is an oscillator, which provides direct d.c. power to RF signal conversion and allows the generated signal to be locked to an external source. Such direct d.c. to RF conversion at the fundamental frequency of oscillation cannot happen at frequencies above f_{max}.

Integrated electronic device technology in III–V and silicon. In the pursuit of increasing f_{max} to increase the amplification range, both silicon-based devices (CMOS, SiGe:SiGeC or bipolar-CMOS (BiCMOS)) and III–V devices (for example, InP HEMTs and HBTs) have made considerable progress. While this Review Article does not focus on the material, device and fabrication level challenges, it is useful to know the state of the f_{max} metrics across the technology landscape. In this, III–V devices have fared better. InP-based HEMTs have reached f_{max} of 1.5 THz, enabling the first solid-state amplifier beyond 1 THz (ref. [66]) (Fig. 2b). In addition, other III–V devices with higher driving capability and breakdown voltages have also crossed into the THz region, such as double-heterojunction bipolar transistors (DHBTs; $f_{max} \approx 1.15$ THz (refs. [18,67])), InP-GaAsSb DHBTs ($f_{max} \approx 0.78$–1.18 THz (refs. [68,69])) and GaN ($f_{max} \approx 0.58$ THz (refs. [18,70])).

Silicon-based technology, particularly CMOS, offers higher levels of integration, but suffers from lower f_{max}, typically in the range of 300–350 GHz (refs. [20,71]). The metric has not improved with size scaling even to the 14 nm node and below in FinFET transistors due to limitations related to parasitics and contact resistances[21]. However, state-of-the-art Si/SiGe:C HBT processes that allow co-integration of CMOS devices have reached peak f_{max} of 0.36 THz (ref. [72]) and up to 0.46 THz range in a commercially available process[73]. In fact, HBTs with f_{max} reaching up to 0.72 THz have also been demonstrated[19,74,75]. This progress is extremely promising as it can simultaneously allow energy-efficient complex signal processing in CMOS with the THz operation in SiGe. The challenge is to scale these device-level experimental demonstrations to wafer-level processing with the tight process control required for high yield on complex integrated systems.

THz signal generation above f_{max} and THz phased arrays. While our discussion so far has focused on f_{max} as a metric for classifying solid-state technology, this is by no means the only important

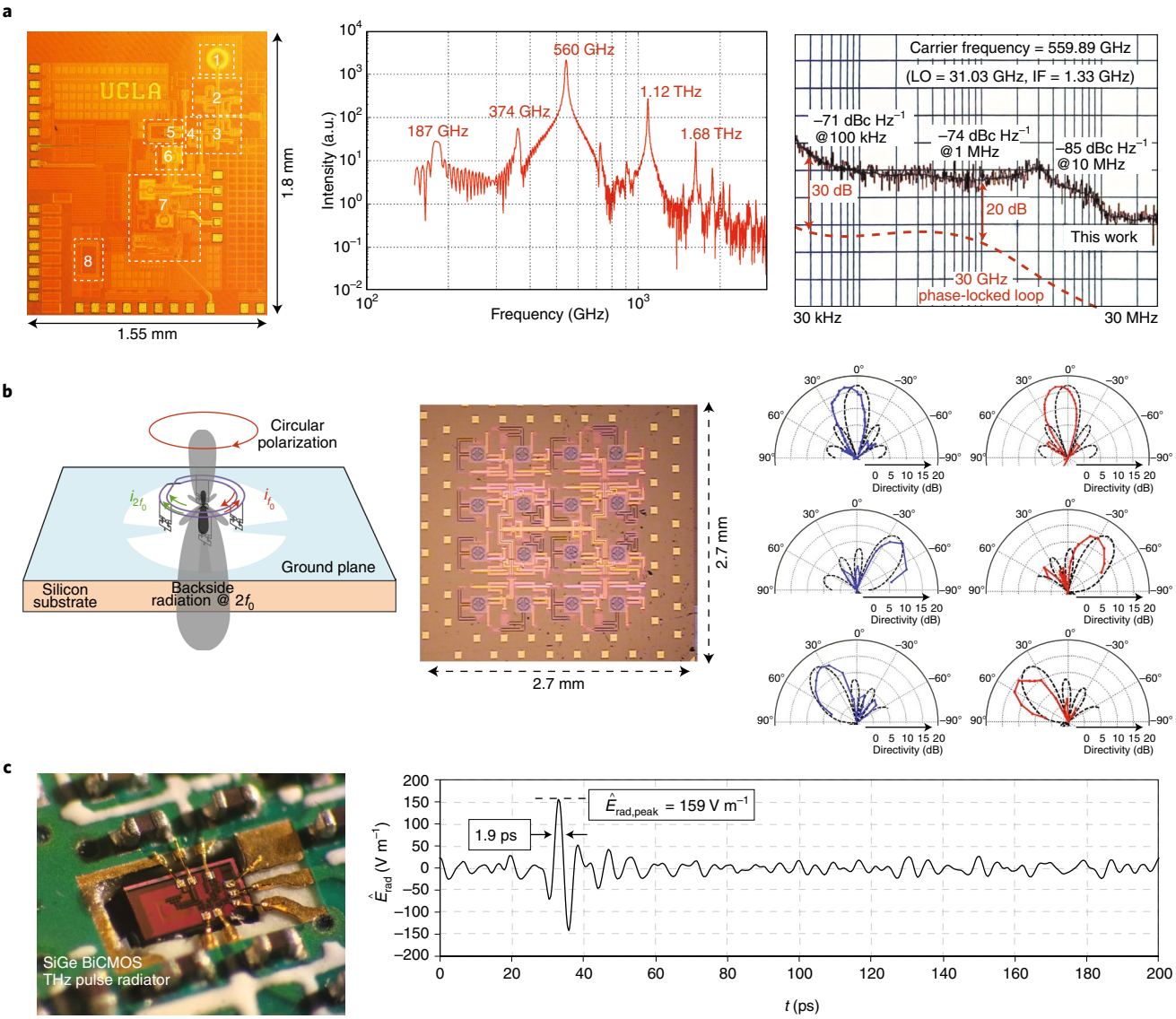

Fig. 3 | THz sources and systems in silicon. a, Fully integrated THz phase-locked loops in CMOS where the fundamental and the harmonic signal (at 0.56 THz) is locked to an external low phase-noise reference[83]. LO, local oscillator; IF, intermediate frequency. **b**, Multifunctional active electromagnetic structures allowing direct conversion of d.c. power to generation and radiation of filtered THz harmonic signal[76]. i_{f_0} and i_{2f_0} represent the filtered fundamental and radiated second harmonic currents, respectively. A 4×4 array in a single chip demonstrated THz phased array operation at 0.28 THz. In the rightmost panel the dashed and solid lines represent simulated and measured data, respectively. **c**, THz picosecond pulse generator in silicon that allows direct digital-to-THz impulse conversion and radiation with on-chip antennas[89]. $\hat{E}_{rad}$ represents the radiated electric field at a distance of 1 cm from the chip. Panels adapted from: **a**, ref. [83], IEEE; **b**, ref. [76], IEEE; **c**, ref. [89], IEEE.

metric to consider. Others include noise figure, 1/f noise corner, breakdown voltages, current driving capability and thermal stability. All of these parameters affect the entire stack from block-level to system performance, impacting the quality (phase noise) of THz signal synthesis, the sensitivity and dynamic range of THz receivers and imagers, and the power generation and handing capability for THz sources.

The impact of silicon-based integrated circuit technology (for example, CMOS, BiCMOS) operating beyond 0.3 THz is only about ten years old, dating to the first demonstrations of signal generation and radiation in 2008 (refs. [59,60]). Since these early works, the field of silicon-based THz circuits and systems have progressed at a breakneck pace and have shown remarkable advances. These include fully integrated phased arrays with tens of mW of effective isotropic radiated power (EIRP) across 0.3–1.0 THz (refs. [61,63,76]), active imaging systems[77], integrated THz camera with over 1,000 pixels[78] and fully integrated THz wireless chipsets with multi-Gbps wireless links[79,80]. This suggests that silicon devices can provide useful functionality above f_{max}. While f_{max} denotes the frequency above which power amplification and self-sustained oscillation can no longer be achieved, this does not imply that it marks the end of the road for integrated circuits. Nonlinearities inherent in device operation can be exploited to generate harmonic power and detect signals beyond f_{max}. This allows the fundamental oscillatory source to be below f_{max} and be locked externally. This indirectly locks the harmonically generated THz signal as well.

For efficient THz signal generation, it is important to push the fundamental frequency very close to f_{max}. This remains challenging since classical oscillators veer far away from the optimal loading conditions needed for optimal power amplification (Fig. 2). To address this challenge, topologies have been demonstrated that pushed oscillator frequencies close to f_{max} with appropriate amplitude

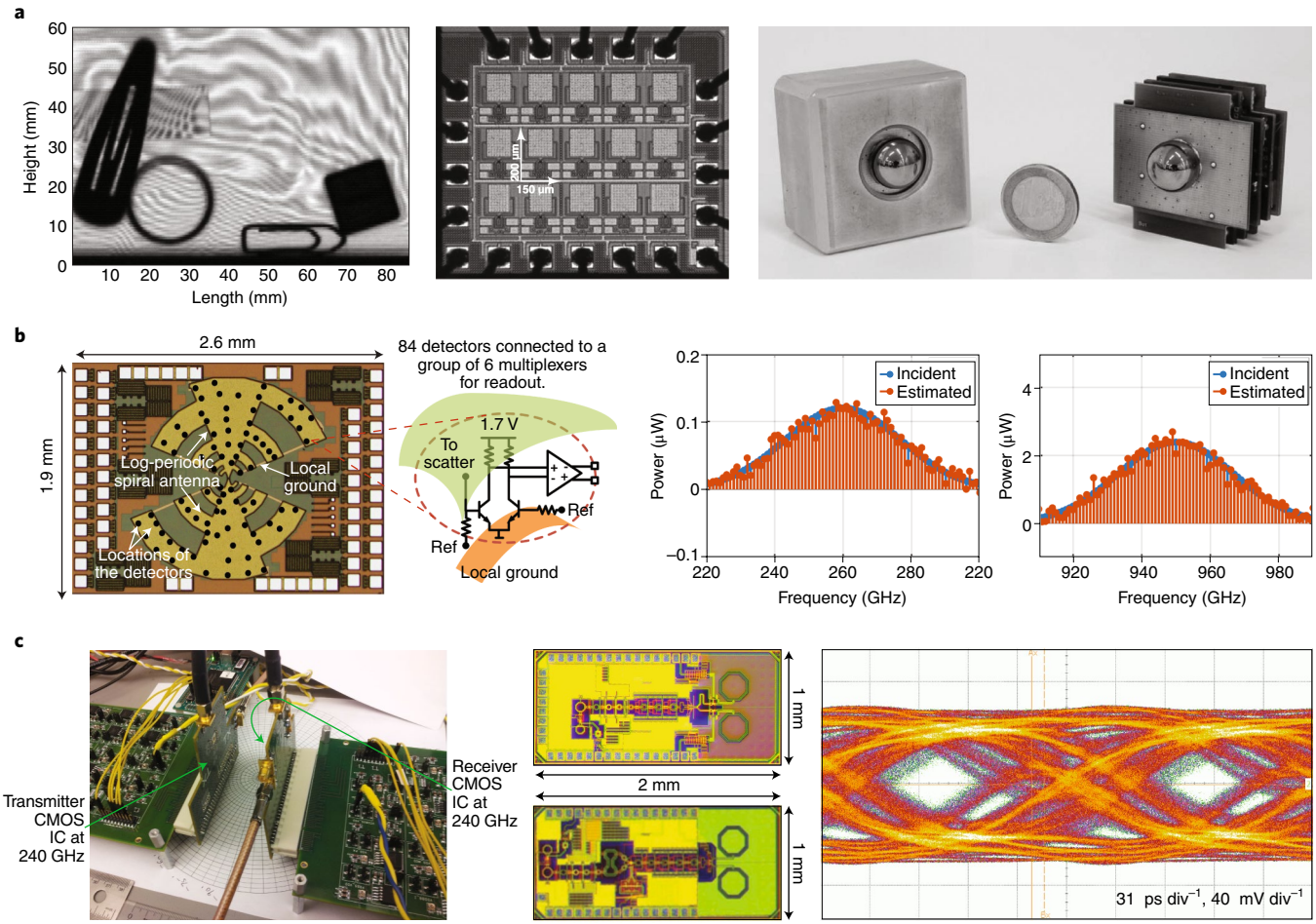

Fig. 4 | THz sensors and receivers in silicon. a, One of the earliest demonstrations of THz imaging in silicon with a 3×5 pixel array in 0.25 μm CMOS operating at 0.65 THz (ref. [97]). The figure also shows a 1,000 pixel THz camera operating in video mode from 0.7 to 1.0 THz (ref. [78]). **b**, Integration of active devices and antennas on the same substrate allows new chip-scale architectures that can exploit deep subwavelength sensing. The figure shows a single-chip THz spectroscope that extracts incident THz spectral information from spatial sensing of scattered fields with integrated devices. Eliminating all complex THz sources, the chip employs regression analysis to allow source-free spectral estimation across 0.04–0.99 THz (refs. [102,103]). **c**, Fully integrated silicon transceivers operating at 0.24 THz with data rates approaching 16 Gbps with phase modulation schemes such as QPSK[105]. Panels adapted from: **a**, left and middle images, ref. [97], IEEE; **a**, right image, ref. [78], IEEE; **b**, ref. [103], Optical Society; **c**, ref. [105], IEEE.

and phase conditions[81]. In addition, the triple stage topology (Fig. 2c) filters the fundamental and second harmonic and allows coherent combination of the filtered third harmonic at the extraction node. Similar symmetries can be exploited to extract higher harmonics such as the fourth (~1 THz (ref. [61])), but the power decreases dramatically. Tunability of the source[64,82] is also critical to enable frequency and phase locking to a low phase-noise reference signal. Phase-locked loops operating at 0.3–0.56 THz have been demonstrated in CMOS (Fig. 3a). These can serve as a frequency reference for massively scaled arrays for both transmitters and imagers[83,84].

Unlike at lower frequencies, a THz signal generated on chip can be radiated out with integrated antennas, enabling compact and simplified packaging. This is a critical feature since extraction of THz signals is otherwise nontrivial, in part due to the sensitivity to parasitics. In such radiating sources, the EIRP is a useful metric as it combines both total radiated power and directivity of the radiated beam. EIRP is defined as $\mathrm{EIRP}(\theta, \varphi) = P_{rad} D(\theta, \varphi)$ where P_{rad} is the radiated power, $D(\theta, \varphi)$ is the directivity of the radiation pattern and θ and φ are the elevation and azimuthal angle in space, respectively. Combining parametric frequency conversion with integrated antennas, silicon-based radiating frequency multipliers have been demonstrated at frequencies reaching up to 1.4 THz (refs. [62,85]).

Exploiting radiating surfaces and integrated devices in the same substrate, one can also engineer new forms of multifunctional electromagnetic surfaces to allow subwavelength control. Such direct synthesis of radiating fields can break many of the trade-offs of the partitioned block-by-block design approach. An example shown in Fig. 3b is a multifunctional active electromagnetic structure that converts d.c. to filtered THz radiated waves by synthesizing optimal currents on the chip surface at the fundamental and desired harmonics. The structure behaves as a resonator for a travelling wave oscillation at the fundamental (f_0) and a selective frequency multiplier, and also as a radiator for $2f_0 > f_{max}$. While the power generated by one single source is limited by the breakdown voltages and device size, several sources can be combined coherently in free space to generate higher power and EIRP. Of course, one must ensure frequency locking and phase coherence among all the sources. In Fig. 3b, a centrally locked 4×4 array with individual phase control allowed beam forming and beam scanning in 3D space with +9.4 dBm EIRP, demonstrating the first phased array near 0.3 THz in silicon[76].

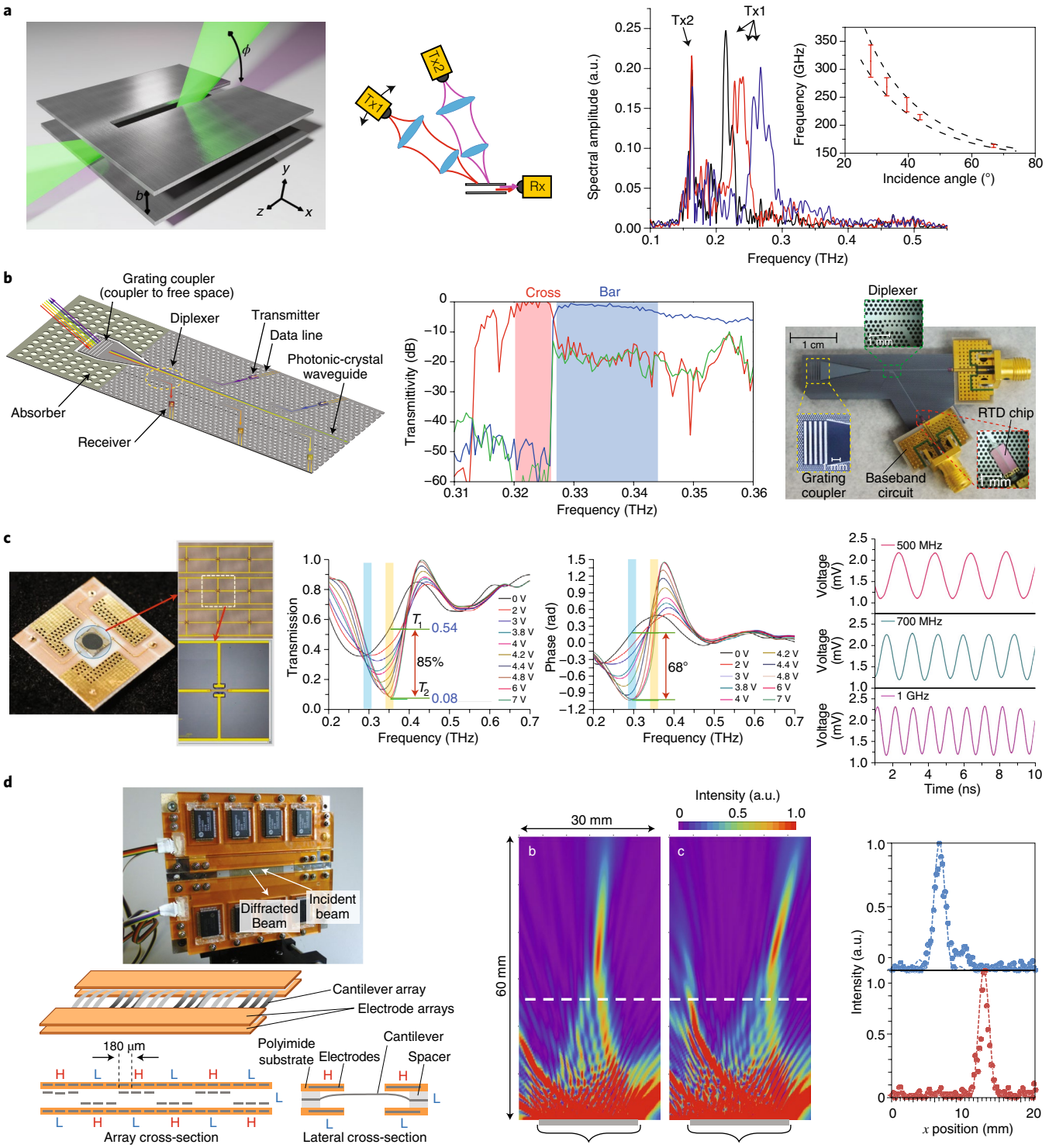

Fig. 5 | Photonics-inspired passive and active THz components. a, Multiplexing of THz signals for distributed signal distribution. Two different transmitters are used to illuminate the waveguide simultaneously with broadband radiation. The multiplexed signal shows two peaks with their centre frequencies determined by the input angles of the two in-coupled beams, respectively[110]. Tx1, transmitter 1; Tx2, transmitter 2; Rx, receiver. **b**, Photonic-crystal inspired THz diplexer[112]. **c**, Unit cell of a composite metamaterial-based THz modulator that combines an equivalent collective dipolar array with a double-channel heterostructure for ultrafast and all-electronic THz modulation. The figure also shows frequency-dependent transmission and phase shift of THz time-domain spectroscopy at different voltages and detection of modulated THz waves[126]. **d**, THz beam forming with a programmable diffraction grating using a linear array of electrostatically actuated cantilevers[129]. H, high; L, low. Panels adapted from: **a**, ref. [110], Springer Nature Ltd; **b**, ref. [112], Optical Society; **c**, ref. [126], American Chemical Society; **d**, ref. [129], Optical Society.

Scalable arrays can also be enabled through mutual injection locking among an array of free-running radiating oscillators[86], or by wireless injection locking to another source[87]. Such locked arrays with hyper-hemispherical lenses can lead to very sharp high-power THz beams[88]. For example, Hu et al. recently demonstrated the first 2D phased array beyond 1 THz, with reported 13 dBm of EIRP[61].

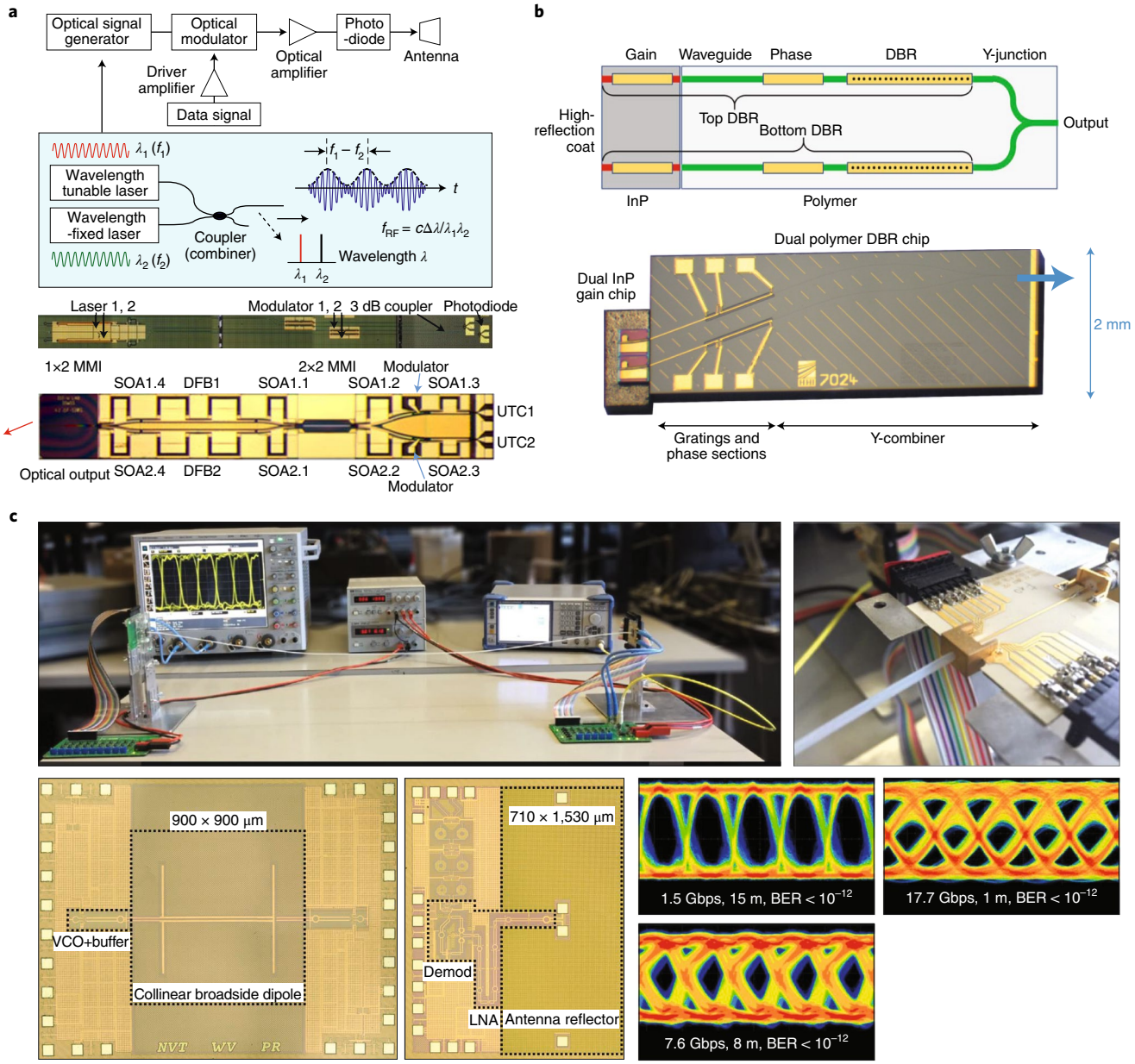

Fig. 6 | Electronic–photonic hybrid THz systems. a, Photonics-based transmitter for THz wireless communications. The chip photographs show a fully integrated microwave and THz signal generator on heterogeneous silicon/III–V (ref. [142]) and on InP substrates[143]. MMI, multimode interference reflectors; SOA, semiconductor optical amplifier. **b**, Dual wavelength source chip with hybrid integration. The figure shows the gain sections on InP and various elements on the polymer substrate such as passive waveguides, phase shifters and DBR sections. The photograph shows the dual hybrid InP/polymer DBR[145]. **c**, Fully integrated CMOS chipsets operating at 0.12 THz with THz plastic waveguides establishing connectivity of 17.7 Gbps over 1 m and 1.5 Gbps over 15 m distance[146,147]. VCO, voltage-controlled oscillator; LNA, low-noise amplifier. Panels adapted from: **a**, upper chip image, ref. [142], Optical Society; **a**, lower chip image, ref. [143], IEEE; **b**, ref. [145], Springer Nature Ltd; **c**, top-left image and two bottom-left images, ref. [146], IEEE; **c**, top-right image and three bottom-right images, ref. [147], IEEE.

Beyond continuous waves, broadband picosecond pulses can also be generated directly in silicon[89]. Here, the digital signals can be directly converted to THz pulses with very fast switching and radiating the stored energy in a manner similar to the spark-plug operation of Marconi-era radios[89] (Fig. 3c). In addition, the time evolution of such picosecond pulses can also be programmed digitally, which enables spectral control of the THz pulses for spectroscopic and imaging applications[90].

THz detection, imaging and fully integrated systems. The ability to generate signals at harmonic frequencies beyond f_{max} also translates to being able to detect signals above f_{max}. Once again, this is accomplished by exploiting the nonlinearities of the devices. The principle of operation is different for SiGe-based bipolar devices and field-effect transistors, and the latter has been shown to detect signals well beyond 3 THz (refs. [91,92]). In the 1990s, Dyakonov and Shur introduced a non quasi-static plasma-wave detection theory that involves plasma-wave generation in the channel by an external THz field interacting with a 2D electron gas in a field-effect device[93,94]. Subsequently, detection experiments have demonstrated both resonant and non-resonant models for rectification of THz signals[95,96]. One of the first demonstrations of focal plane array at THz in an

Table 1 | Summary of advancements and state of the art in THz devices, circuits and systems across electronics, photonics and hybrid approaches

	Devices, circuits and systems	Description and representative examples
Devices	III–V	InP HEMTs (f_{max} ~ 1.5 THz)[66], InP DHBTs (f_{max} ~ 1.15 THz)[18,67], InP-GaAsSb DHBT (f_{max} ~ 0.78–1.18 THz)[68,69], GaN (f_{max} ~ 0.58 THz)[18,70]
	Silicon	CMOS (f_{max} ~ 0.3–0.35 THz)[20,71], Si/SiGe:C HBT (f_{max} ~ 0.46–0.50 THz)[19,73], experimental Si/SiGe:C HBTs (f_{max} ~ 0.72 THz)[19,74,75]
Solid-state electronics (III–IV, silicon)	III–V/Schottky diode-based sources	248 mW (0.2 THz)[45], 20 mW (0.3 THz)[44], 2 mW (0.6 THz)[46], 60 μW (2 THz), 18 μW (2.6 THz)[39,40]
	Silicon-based sources (oscillators, frequency multiplier, synchronized sources on-chip)	3.3 mW (0.3 THz)[63], 1 mW (0.5 THz)[64], 100 μW (1 THz)[61], 50 μW (1.4 THz)[62]
	Phase-locked loops	0.56 THz phase-locked loop, −74 dBc Hz^{-1} at 1 MHz offset (phase noise)[83]
	Phased arrays	16-element, +9.4 dBm EIRP (0.28 THz)[76], 2×4 element, 24.4 dBm EIRP (silicon lens, 0.55 THz)[88], 42-element array, 13 dBm EIRP (silicon lens, 1 THz)[61]
	THz imaging (coherent and non-coherent)	16-element array, 70 pW sensitivity (1 kHz bandwidth, 0.32 THz)[77]; 1,024 pixels (0.7–1.1 THz), 12 nW sensitivity (500 kHz bandwidth, 0.86 THz)[78]
	THz imaging (near-field)	Near-field sensor at 0.55 THz with 10–12 μm resolution[104]
	Spectroscopes	0.04–0.99 THz (refs. [102,103]), 0.22–0.33 THz (ref. [152])
	Wireless communication	16 Gbps at 0.24 THz with integrated CMOS chipsets separated by a distance of 2 cm and a measured BER of 10^{-4} (ref. [105])
Photonics-inspired components	Waveguides, splitters, diplexers	Parallel-plate waveguides[107], rectangular waveguides[108], power splitter (0.2–0.3 THz)[109], 3D-printed dielectric waveguide (0.12 THz)[111], photonic crystal-based diplexer[112]
	Multiplexers/demultiplexers	Leaky-wave antenna based on the parallel-plate waveguide (0.1–0.5 THz)[110]
	Filters, isolators, polarizers	Dielectric and metal-stack-based structure (~0.1–0.5 THz)[117–119]
	Tunable filters	Liquid metal-based[120], microelectromechanical systems (~0.48–0.68 THz)[121], gated-graphene devices (~0.6 THz)[122]
	Modulators	Electrically driven THz metamaterial diffractive modulator (~0.4 THz)[125], III–V heterostructures with metasurface arrays (GHz speed at 0.35 THz)[126], tunable THz slot waveguide (0.25 THz)[127]
	Beam steering	Electrostatically actuated cantilevers (0.15–0.9 THz)[129], liquid crystals (0.3–0.6 THz)[130]
	Antenna innovations	Graphene antennas (1 THz) for reconfigurable MIMO[131,132], plasmonic antenna arrays[133]
Electronics–photonics hybrid systems	Microwave frequency synthesizer	Fully integrated microwave frequency synthesizer on heterogeneous silicon/III–V (1–112 GHz)[142]
	Optical phased locked loop	Optical phase-locked loops (photonic integrated circuits and off-the-shelf electronics)[144]
	Wireless communication	Photomixers (such as UTC diodes), Schottky-barrier diodes[136,137], tunable hybrid photonic/THz systems[145], Hybrid electronics–photonics-based wireless links (100 Gbps over 3 channels at 237 GHz over 20 m (ref. [136]) and 260 Gbps over 6 channels[141]
	Wireline communication	Plastic waveguide at 0.12 THz and CMOS multi-Gbps transceivers (1.5 Gbps over a length of 15 m)[147]

industry standard CMOS technology was by Öjefors et al.[97] where a 3×5 array THz imager with integrated antenna and detector serving as individual pixels was fabricated in a 0.25 μm process (Fig. 4a). The device operated at 0.65 THz, nearly four to five times the cut-off frequency, and yet still achieved a high sensitivity of 300 pW $\sqrt{Hz^{-1}}$. Since these early works, tremendous progress has been made in THz imagers including 1,000 pixel THz video-rate imaging from 0.7 to 1.0 THz (ref. [78]) (Fig. 4a), hyper spectral imaging from 0.16 to 1.0 THz (refs. [98,99]), CMOS-integrated Schottky diode imagers at 0.86 THz (ref. [100]) and an all-silicon imaging chipset at 0.28 THz (ref. [101]).

In a manner similar to the subwavelength synthesis of THz fields with circuits, subwavelength sensing has also been shown to allow fully integrated spectroscopic chips operating across 0.04–0.99 THz without the need for any external THz source[102,103] (Fig. 4b).

Coherent detection allows phase discrimination capabilities. Three-dimensional imaging and fully coherent integrated imaging systems, and even near-field imaging systems, have been demonstrated in silicon at 0.32 THz (refs. [77,104]). In short-range communication, fully integrated THz transmitter–receiver systems have been demonstrated at 0.24 THz (refs. [105,106]) with the data rates of the

former reaching up to 16 Gbps with quadrature phase-shift keying (QPSK) modulation. At a separation distance of 2 cm, the chipset establishes a bit-error-rate (BER) of 10^{-4} (Fig. 4c).

Clearly, many key functionalities have been demonstrated in integrated circuits, with capabilities such as beam forming for applications in sensing, imaging and communication. However, much work needs to be done to enable fully functional THz systems, which may require transport of THz signals across longer distances between integrated circuits, multiplexing and demultiplexing across a network of nodes or even free-space modulation, and so on. So far, most of these demonstrations have been undertaken in the domain of photonics-inspired research.

Electronic–photonic hybrid approach

The propagation of THz signals is quite different from that of signals at lower frequencies, in a number of ways. These differences offer both challenges and opportunities for system design. Most notably, THz signals are generally much more directional, propagating as diffracting beams rather than omnidirectional broadcasts. In this way, THz signals are more similar to laser beams than to RF wireless links. Because of this high directionality, one can easily envision system configurations in which signal processing functions are separated from the source and/or detector subsystems. Taking inspiration from the realm of optics and laser science, many researchers have been pursuing the demonstration of specific device functions. In many cases, these devices are agnostic with respect to the particular choice of radiation source and could therefore be integrated into a wide range of different system configurations. The versatility afforded by this approach may offer significant advantages in the design of flexible and power-efficient architectures. Here, we discuss a few examples that illustrate the breadth of materials and concepts that have been studied in recent years.

Photonics-inspired components. One obvious need in most THz systems is signal transport. In cases where free-space propagation is impractical, waveguides offer a valuable alternative. Of course, conventional waveguide structures for lower frequencies can often be scaled to the THz range. However, in many cases, it is desirable to preserve the broad bandwidth and low dispersion of a free-space link, criteria that are often not compatible with conventional waveguide geometries, especially those that are integrated on substrates. As a result, most waveguide research in the THz range has relied on bulk metal components, such as parallel-plate metal waveguides[107] or rectangular metal waveguides[108]. In addition to offering low-loss propagation of THz signals, these waveguides can provide a number of options for versatile signal processing. For instance, simple waveguide designs can be implemented for tunable power splitting with high dynamic range[109]. Taking advantage of the directional diffraction-limited nature of THz beams, a leaky-wave design based on the parallel-plate waveguide can be used for versatile multiplexing and demultiplexing of THz signals[110] (Fig. 5a). Other waveguide structures, based on 3D-printed polymer components[111] or silicon-based photonic crystal structures[112] (Fig. 5b), can provide additional passive functionality, and are generally compatible with high-speed data transmission[113].

Filters provide another important capability for signal processing. In the THz range, many passive filter options are available in the form of bulk optical components, drawing from a long history of research work in optical interference filters or frequency-selective surfaces. At lower frequencies, high quality factor (Q) resonators are often employed for very narrowband filtering. In the THz range, this strategy is not yet well established because of significant fabrication challenges as well as intrinsic material losses that limit the achievable Q factor of an integrated resonator. However, there is significant interest in such structures[114,115], both for THz signal processing and as tools for the study of fundamental quantum optics[116].

Researchers are also pursuing other options, inspired by free-space optics. For instance, a stack of waveguides can emulate an artificial dielectric medium, offering tremendous versatility and very low passive losses. This idea of an artificial dielectric based on stacked metal waveguides was first considered over 60 years ago, but finds new life in the THz range where the size scaling enables practical and efficient devices[117]. Two stacks of uniformly spaced metal plates can be arranged to emulate the spatial dispersion of a four-prism sequence, commonly used for dispersion control in ultrafast optics. This can therefore provide almost arbitrary filtering capability for free-space THz beams[118]. This stack-of-waveguides concept can also be employed for a variety of other functions, including polarization control and passive isolation[119].

Active devices are also attracting increasing attention for filtering of THz signals. For example, two closely spaced metal waveguides, with parallel propagation axes, can be coupled by a small gap containing a liquid-metal-filled capillary. This gap mediates the electromagnetic coupling between the waveguides. The spectral bandwidth of the coupling depends on the size and geometry of the coupling region, and the coupling efficiency can be tuned through the electrically controlled repositioning of the liquid metal. This scalable and efficient filter configuration can enable important capabilities such as channel add–drop[120]. Reconfigurable microelectromechanical system devices provide another option for efficient and low-power electrically switched filters. Electrostatic actuation of in-plane microelectromechanical system switches can be used to change the electromagnetic response of a metasurface array, providing a tunable filter at kHz rates[121]. Other examples include electrically gated graphene-based devices, which are attracting a great deal of attention for reconfigurable THz optoelectronics[122].

Another key example is that of external modulators. Early work on free-space THz modulators based on switchable metasurfaces using simple III–V devices[123] has been followed up by a flood of work aimed at achieving improved switching speeds, modulation contrast and insertion losses. Higher modulation depth can be achieved by integrating a gated graphene layer with a passive ridge waveguide[124], or by exploiting a metasurface monolayer in a diffractive geometry, similar to conventional acousto-optic modulators[125]. The integration of more sophisticated III–V heterostructures with metasurface arrays[126] or on-chip slot waveguides[127] can provide a switching element with high speed and high modulation depth, and with low power consumption (Fig. 5c). Because of the high directionality of THz beams, most THz systems will require the capability to steer the beam. Of course, beam steering can be achieved with an array of phase-stable sources, which can be integrated on-chip[128]. However, as with the above examples, there are advantages to separating the source subsystem from the signal processing component. Researchers have demonstrated several possible configurations for electrically actuated external beam-steering devices. For example, Monnai and colleagues fabricated a programmable diffraction grating using a linear array of electrostatically actuated cantilevers[129] (Fig. 5d). Other researchers have explored the use of liquid crystals for beam steering. Using a wedge-shaped cell, a transmitted THz beam can be refracted to different angles by electrical control of the liquid-crystal alignment[130]. Even so, this remains one of the thorny unresolved device challenges for THz systems.

In the context of THz communications systems, antennas offer another set of challenges. As with most of the aforementioned examples, the field of antennas is rich, with a great deal of earlier work on which to build[131]. It is generally recognized that multi-input–multi-output (MIMO) antenna systems will be a critical component of future THz wireless systems; indeed, the possibility of building compact phase-coherent MIMO arrays is one of the key advantages for THz communication systems over free-space optical communications. Still, many open questions remain about implementation and optimization. New materials such as graphene

may enable novel MIMO architectures[132,133], which exploit the deep subwavelength confinement of plasmonic excitations to achieve a large number of antennas in a small footprint. Such arrays could be used for beam forming as well as spatial and spectral multiplexing. However, the nature of THz signal propagation also gives rise to new challenges, not typically faced by more familiar RF systems. For example, a diffracting THz beam may propagate in a slightly different direction from that of its modulation sidebands, as diffraction angles depend on frequency[134]. This implies that different elements in a MIMO array may detect different modulation information even if all paths are direct line-of- sight. This situation will require a new approach to the extraction of data from measured signals. The data analysis will become even more complex in the presence of non-line-of-sight channels, which are feasible in some situations, even at frequencies up to 400 GHz (ref. [135]).

Electronics–photonics hybrid systems. The ability to manipulate THz fields in passive devices can be combined seamlessly with photonic integrated circuit technologies to enable photonic chipsets with enhanced THz capability. As a key example, in wireless communication systems, such photonic techniques can be employed in the transmitter, where two different light sources, an optical amplitude/phase modulator, and a high-power output photomixer like a uni-travelling-carrier (UTC) photodiode can be used to generate continuous THz waves via a heterodyne mixing process (Fig. 6a). Highly sensitive receivers can be realized with all-electronic devices such as Schottky-barrier diodes[136,137] or other solid-state receivers. It should be noted that this method exploits many photonics–electronics hybrid components that are readily available with telecom-based high-frequency devices, including optical fibre cables. The use of optical fibre also enables the distribution of high-frequency RF signals over long distances, and makes the size of transmitter front ends compact and light. Moreover, a significant advantage of the photonics-based approach is that wired (fibre optic) and wireless communication networks could be connected seamlessly in terms of data rates and modulation formats. Frequency-division multiplexing multichannel systems can be easily realized using multiwavelength laser sources developed for optical wavelength-division multiplexing networks. Using this approach, single channel data rates of 50 Gbps (error free) with on–off keying (OOK) at 0.32 THz (ref. [138]), 90 Gbps (real time, bit error rate (BER) = 10^{-4}) with QPSK at 0.32 THz (ref. [139]), 106 Gbps (with offline digital signal processing (DSP), BER = 10^{-4}) with 16-quadrature amplitude modulation (16-QAM) at 0.4 THz (ref. [140]) have been achieved. With multichannel systems, data rates up to 260 Gbps have been demonstrated[141].

To compete with all-electronic and integrated circuits-based THz transceiver technologies, there have been several studies on the integration of both monolithic and hybrid photonic components. With a hybrid integration scheme, the performance of each component can be optimized more easily than the monolithic integration. For example, a fully monolithically integrated transmitter, which consists of two lasers, optical amplifiers, an optical intensity modulator and photodiodes, was fabricated on Si (ref. [142]) and InP (ref. [143]) substrates (Fig. 6a). Optical injection locking and optical phase-locked loop techniques were introduced for phase stabilization[144]. Figure 6b shows another hybrid example of a dual-wavelength photonic source, which consists of gain sections on InP and the elements on the polymer substrate, including passive waveguides, phase shifters and distributed Bragg reflector (DBR) sections. Frequency tuning of over 4 THz is feasible with this chip[145]. Another example that highlights this electronic–photonic hybrid approach is the use of a plastic waveguide to carry THz waves at 0.12 THz over long distances, with fully integrated CMOS chipsets interfacing to both ends (Fig. 6c). The plastic waveguides overcome the losses associated with copper-based interconnects over long distances, leveraging the low loss of the dielectric waveguide, and demonstrated an error-free data rate of 1.5 Gbps over a length of 15 m. This approach that is inspired by an electronic–photonic hybrid system can allow efficient multi-Gbps links in large data centres[146,147]. The co-design approach across electronics and photonics, whether on a single heterogeneous integrated platform or as multi-chip modules, is expected to play a major role in very-high-performance THz systems, particularly focusing on THz wireless communication[137]. The notable advancements in THz devices, circuits and systems across electronics, photonics and hybrid approaches and the current state of the art are summarized in Table 1.

Future of THz integrated systems

The development of THz integrated systems will be greatly impacted by the applications that develop in the next decade. The capabilities of THz imaging and sensing are promising for non-destructive quality control, 3D imaging, radar, and gesture recognition in autonomous systems, vehicles, robotics and industrial automation, particularly in the lower part of the spectrum (~0.1–0.3 THz). Given the need for compact, efficient, high-performance sensing devices, operable at low power and deployable at large scale, integrated circuit technology must play a major role. We expect that the device performance in silicon, particularly SiGe-based devices, will continue to improve with f_{max} reaching up to, or perhaps exceeding, 1 THz in the next decade. At higher frequencies beyond 1 THz, it is likely that the solution will be heterogeneous, with the front-ends being realized in III–V technology and the rest of the system in silicon. This could be implemented with separate chips packaged in multichip modules, or with 3D-stack integrated circuits and III–V/silicon heterogeneous integration in which there have been promising developments in recent years. The technology of choice will depend on the application, which at THz, can be particularly diverse spanning from sensing, spectroscopy and imaging to wireless communication.

The foremost challenge to enable real-world applications in THz sensing, spectroscopy and imaging is the need for efficient and widely reconfigurable chip-scale systems (in properties such as spectrum, radiation patterns and polarization), as we have emphasized in this Review Article. The THz range is rich in spectroscopic features. For years, it has shown promising capabilities, but its deployment has been limited due to the complexity of the technology at hand. The two most prominent examples involve the relatively narrow absorption lines of rotational or ro-vibrational excitations in gases, and the somewhat broader lines that result from lattice vibrations (phonons) in crystalline solids, especially in molecular crystals[148]. As a result, one can envision using THz spectroscopy for identification of the chemical composition of powders[149] or plumes[150], for example. The absorption strength of many polar molecules peaks in the THz range, and numerous techniques have been developed recently to enhance the sensitivity and specificity of gas sensing[151]. As with mid-infrared fingerprint spectroscopy, the ability of a sensor to offer both highly specific and sensitive detection relies crucially on the tuning range of the system, among other parameters. One of the key challenges for THz spectroscopic sensing is that the spectral lines of interest are often broader or more widely spaced than the tuning range of typical solid-state sources. New developments in broadly tunable solid-state sources would prove extremely valuable in this context. Some recent works have shown promising advancements in this regard. This includes a fully integrated spectroscope across 220–330 GHz in silicon with a reported minimum detectable concentration of 11 ppm for carbonyl sulfide (OCS)[152]. Other works have circumvented the need for a tunable THz source to enable extremely wide spectral estimation (0.04–0.99 THz). This is done by spatially sampling the near fields on the capture antenna, and applying estimation techniques and regression analysis for source-free spectral sensing[103].

THz imaging can also gain a more a solid footing particularly at frequencies in the range of 100–300 GHz in the coming decade. In combination with millimetre-wave frequencies, hyperspectral imaging at THz can allow for 3D imaging with both high lateral and depth resolution. We are seeing a similar evolution in the neighbouring spectra, where sensor fusion particularly combining millimetre-wave, infrared and optical frequencies is becoming a critical sensing tool in autonomous vehicles and systems. Similar advancements can occur at THz with multispectral sources. Previous works on chip-scale sources with dynamically programmable spectral content is promising in this regard[90]. But, the challenge to create widely reconfigurable sources with the capability of beam forming for fast image acquisition still remains. Computational-based imaging techniques, which have been demonstrated at millimetre-wave frequencies, can emerge as an alternative mechanism to scanning for real-time imaging[153,154]. In combination with machine learning and deep neural networks for real-time feature extraction, this can be an enabling feature in quality control and security-based imaging. Irrespective of the exact application and methodology, it can be understood that for real-world applications in THz sensing and imaging, widely reconfigurable, efficient, scalable and low-cost technology remains a foremost, and potentially rewarding, challenge.

However, we also see a strong potential for THz in wireless communication, for wireless backhaul replacing the last mile of optical fibre, for wireless links in data centres, and for other short range and high bandwidth applications. The unique propagation, scattering and diffraction characteristics of THz waves, and simultaneous limitations of the device technology, open up new challenges across the various levels of abstraction. This ranges from circuits and communication architecture to channel estimation, equalization, interference and resource management through networking and protocols. There are valuable lessons to be learnt from the sister millimetre-wave bands where there is an expected densification of base stations and wireless backhauling for the fifth generation (5G) of cellular connectivity. The potential was identified by the Institute of Electrical and Electronics Engineers (IEEE), which formed the IEEE 802.15.3d task force to investigate the spectral allocations and standardizations of the physical and medium access control (MAC) layer across 252–325 GHz. The use case scenarios include kiosk downloading, intrachip/intraboard radio communication, wireless communication in data centres and mobile front and backhaul links. The IEEE 802.15.3d-2017 (ref. [155]) is the first IEEE standard that addressed frequency bands beyond the 0.3 THz range, focusing on the 69.12 GHz span across 252.72–321.84 GHz. This is an important milestone, and takes the first step towards proposing spectral sharing in the 275–1,000 GHz span with applications in the Earth Exploration Satellite Service and radio astronomy. The technological challenge of scalable, low-cost interfaces to realize such a network, however, still remains. We note that THz links suffer from high path loss (for example, at 300 GHz and for a distance of 10 m, the factor $(\lambda/4\pi R)^2$ is ~−100 dB). As a result, highly directional THz beams (often with electronic beam steering) supporting wide bandwidths will be necessary in many applications to overcome this loss factor. Large-scale THz arrays can be an enabling technology, but it is still far from becoming efficient and practical. There are some promising advancements in recent years, particularly at frequencies close to 100 GHz, where beam EIRP of ~60 dBm and beam widths with 2–5° have already been demonstrated in silicon with 256-element phased arrays[156]. Such scalability is yet to be demonstrated at frequencies beyond 300 GHz, where efficiency degradation becomes drastic due to the f_{max} limitations of the devices.

Large-scale THz arrays can find applications in satellite communication, as extremely high gain links can be realized in smaller satellites at THz frequencies (as an example, ~70–75 dBi in 1 m diameter antennas at 0.6 THz)[157]. They have an advantage over free-space optical links due to their scanning ability and automatic alignment. As an increasing number of low- and medium-orbit satellites get deployed for future connectivity, such high-capacity THz links can serve as a supporting mesh network in the future.

In contrast, for short-range high-capacity links in indoor applications, compact THz hotspots can enable a new class of femtocell devices. They can be used flexibly for massive data offloading or for serving emerging applications such as virtual and augmented reality, in-home service and automation[158]. High capacity, adaptive short-range THz links can also be utilized to seamlessly augment network capacities in data centres, avoiding the need for complex rewiring to serve exponentially increasing data traffic. Irrespective of whether such links are deployed for indoor or outdoor applications, reliable channel modelling is critical. Accurate statistical modelling based on extensive channel measurements at THz is severely lacking[159]. The importance of this area of research is evident if we look at the millimetre-wave band, where only after extensive channel measurements, it was evident that millimetre-wave outdoor cellular connectivity is possible and potentially game-changing[160].

The suitable technology to enable this diverse set of wireless technology is still an open area of research. While hybrid III–V/silicon is expected to play a major role, photonics-based systems will also be a close competitor in this case. The debate between modulation complexity with lower bandwidth (compatible with semiconductor integrated circuits) and simpler modulation formats (on–off keying) with higher bandwidths (compatible with photonics-based integrated circuits) is still not settled. Beyond 1 THz and extending up to 10 THz, photonics-based systems comprising quantum-cascade lasers, silicon photonics and photomixer devices are expected to play a dominant role, particularly in systems where tunability of more than 1 THz may be needed. In such systems, efficient optical-to-THz, and THz-to-optical converters are key future challenges. As integrated photonics platforms continue to improve with the incorporation of passive devices and active devices, such as high-speed modulators, THz systems will enjoy the ancillary benefits. To enable this heterogeneous future, research pathways across electronics and photonics, which have mostly developed independently, will need to continue to converge.

Received: 29 May 2018; Accepted: 30 October 2018;
Published online: 13 December 2018

References

1. Rubens, H. & Nichols, E. F. Heat rays of great wave length. *Phys. Rev.* **4**, 314–323 (1897).
2. Tonouchi, M. Cutting-edge terahertz technology. *Nat. Photon.* **1**, 97–105 (2007).
3. Siegel, P. H. Terahertz technology. *IEEE Trans. Microw. Theory Tech.* **50**, 910–928 (2002).
4. Duling, I. & Zimdars, D. Terahertz imaging: revealing hidden defects. *Nat. Photon.* **3**, 630–632 (2009).
5. Ferguson, B. & Zheng, X.-C. Materials for terahertz science and technology. *Nat. Mater.* **1**, 26–33 (2002).
6. Song, H. J. & Nagatsuma, T. Present and future of terahertz communications. *IEEE Trans. Terahertz Sci. Technol.* **1**, 256–263 (2011).
7. Siegel, P. H. Terahertz technology in biology and medicine. *IEEE Trans. Microw. Theory Tech.* **52**, 2438–2447 (2004).
8. Mittleman, D. M. Twenty years of terahertz imaging. *Opt. Express* **26**, 9417–9431 (2018).
9. Mittleman, D. M. Terahertz science and technology. *J. Appl. Phys.* **122**, 230901 (2017).
10. Hu, B. & Nuss, M. Imaging with terahertz waves. *Opt. Lett.* **20**, 1716–1718 (1995).
11. Woodward, R. M. et al. Terahertz pulse imaging in reflection geometry of human skin cancer and skin tissue. *Phys. Med. Biol.* **47**, 3853–3863 (2002).
12. Pickwell, E. & Wallace, V. P. Biomedical applications of terahertz technology. *J. Phys. D Appl. Phys.* **39**, R301–R310 (2006).
13. Liu, H.-B. et al. Terahertz spectroscopy and imaging for defense and security applications. *Proc. IEEE* **95**, 1514–1527 (2007).
14. Bolivar, P. H. et al. Label-free probing of genes by time-domain terahertz sensing. *Phys. Med. Biol.* **47**, 3815–3821 (2002).

15. Xie, L., Gao, W., Shu, J., Ying, Y. & Kono, J. Extraordinary sensitivity enhancement by metasurfaces in terahertz detection of antibiotics. *Sci. Rep.* **5**, 8671 (2015).
16. Cooper, K. B. et al. THz imaging radar for standoff personnel screening. *IEEE Trans. Terahertz Sci. Technol.* **1**, 169–182 (2011).
17. Stake, J., Malko, A., Bryllert, T. & Vukusic, J. Status and prospects of high-power heterostructure barrier varactor frequency multipliers. *Proc. IEEE* **105**, 1008–1019 (2017).
18. Urteaga, M., Griffith, Z., Seo, M., Hacker, J. & Rodwell, M. J. W. InP HBT technologies for THz integrated circuits. *Proc. IEEE* **105**, 1051–1067 (2017).
19. Chevalier, P. et al. Si/SiGe:C and InP/GaAsSb heterojunction bipolar transistors for THz applications. *Proc. IEEE* **105**, 1035–1050 (2017).
20. Voinigescu, S. P. et al. Silicon millimeter-wave, terahertz, and high-speed fiber-optic device and benchmark circuit scaling through the 2030 ITRS horizon. *Proc. IEEE* **105**, 1087–1104 (2017).
21. Schröter, M. et al. SiGe HBT technology: future trends and TCAD-based roadmap. *Proc. IEEE* **105**, 1068–1086 (2017).
22. Ju, L. et al. Graphene plasmonics for tunable terahertz metamaterials. *Nat. Nanotech.* **6**, 630–634 (2011).
23. Tassin, P. et al. Graphene for terahertz applications. *Science* **341**, 620–621 (2013).
24. Kazior, T. E. Beyond CMOS: heterogeneous integration of III-V devices, RF MEMS and other dissimilar materials/devices with Si CMOS to create intelligent microsystems. *Philos. Trans. A Math. Phys. Eng. Sci.* **372**, 20130105 (2014).
25. Song, H. J. Packages for terahertz electronics. *Proc. IEEE* **105**, 1121–1138 (2017).
26. Chattopadhyay, G., Reck, T., Lee, C. & Jung-Kubiak, C. Micromachined packaging for terahertz systems. *Proc. IEEE* **105**, 1139–1150 (2017).
27. Vijayraghavan, K. et al. Broadly tunable terahertz generation in mid-infrared quantum cascade lasers. *Nat. Commun.* **4**, 2021 (2013).
28. Sirtori, C., Barbieri, S. & Colombelli, R. Wave engineering with THz quantum cascade lasers. *Nat. Photon.* **7**, 691–701 (2013).
29. Wanke, M. C. et al. Monolithically integrated solid-state terahertz transceivers. *Nat. Photon.* **4**, 565–569 (2010).
30. Hammar, A. et al. Terahertz direct detection in $YBa_2Cu_3O_7$ microbolometers. *IEEE Trans. Terahertz Sci. Technol.* **1**, 390–394 (2011).
31. Liu, L. et al. Development of integrated terahertz broadband detectors utilizing superconducting hot-electron bolometers. *IEEE Trans. Appl. Supercond.* **19**, 282–286 (2009).
32. Peng, K. et al. Single nanowire photoconductive terahertz detectors. *Nano. Lett.* **15**, 206–210 (2014).
33. Gu, J. et al. Active control of electromagnetically induced transparency analogue in terahertz metamaterials. *Nat. Commun.* **3**, 1151 (2012).
34. Grady, N. K. et al. Terahertz metamaterials for linear polarization conversion and anomalous refraction. *Science* **340**, 1304–1307 (2013).
35. Tanoto, H. et al. Greatly enhanced continuous-wave terahertz emission by nano-electrodes in a photoconductive photomixer. *Nat. Photon.* **6**, 121–126 (2012).
36. Heshmat, B. et al. Nanoplasmonic terahertz photoconductive switch on GaAs. *Nano Lett.* **12**, 6255–6259 (2012).
37. Ward, J. S. et al. Tunable broadband frequency-multiplied terahertz sources. In *33rd Int. Conf. Infrared, Millimeter and Terahertz Waves* 1–3 (IEEE, 2008).
38. Porterfield, D. W. High-efficiency terahertz frequency triplers. *IEEE MTT-S Int. Microw. Symp*. 337–340 (2007).
39. Mstrnini, A. et al. Frequency tunable electronic sources working at room temperature in the 1 to 3 THz band. *Proc. SPIE* **8496**, 84960F (2012).
40. Mehdi, I., Siles, J. V., Lee, C. & Schlecht, E. THz diode technology: status, prospects, and applications. *Proc. IEEE* **105**, 990–1007 (2017).
41. Pardo, D., Grajal, J., Pe'rez-Moreno, C. G. & Prez, S. An assessment of available models for the design of Schottky-based multipliers up to THz frequencies. *IEEE Trans. Terahertz Sci. Technol.* **4**, 277–287 (2014).
42. Deal, W. R., Leong, K., Zamora, A., Radisic, V. & Mei, X. B. Recent progress in scaling InP HEMT TMIC technology to 850 GHz. *IEEE MTT-S Int. Microw. Symp*. 1–3 (2014).
43. Leong, K. M. K. H. et al. A 0.85 THz low noise amplifier using InP HEMT transistors. *IEEE Microw. Wirel. Compon. Lett.* **25**, 397–399 (2015).
44. Kim, J., Jeon, S., Kim, M., Urteaga, M. & Jeong, J. H-band power amplifier integrated circuits using 250-nm InP HBT technology. *IEEE Trans. Terahertz Sci. Technol.* **5**, 215–222 (2015).
45. Griffith, Z., Urteaga, M. & Rowell, P. 180–265 GHz, 17–24 dBm output power broadband, high-gain power amplifiers in InP HBT. *IEEE MTT-S Int. Microw. Symp*. 973–976 (2017).
46. Kang, S., Kim, D., Urteaga, M. & Seo, M. State-of-the-art THz integrated circuits in InP HBT technologies. *IEEE Int. Symp. Radio-Freq. Int. Technol.* 25–27 (2017).
47. Brown, E. R. et al. Oscillations up to 712 GHz in InAs/AlSb resonant tunneling diodes. *Appl. Phys. Lett.* **58**, 2291–2293 (1991).
48. Reddy, M. et al. Monolithic Schottky-collector resonant tunnel diode oscillator arrays to 650 GHz. *IEEE Electron Dev. Lett.* **18**, 218–221 (1997).
49. Kanaya, H., Maekawa, T., Suzuki, S. & Asada, M. Structure dependence of oscillation characteristics of resonant-tunneling-diode terahertz oscillators associated with intrinsic and extrinsic delay times. *Jpn J. Appl. Phys.* **54**, 094103 (2015).
50. Maekawa, T., Kanaya, H., Suzuki, S. & Asada, M. Oscillation up to 1.92 THz in resonant tunneling diode by reduced conduction loss. *Appl. Phys. Express* **9**, 024101 (2016).
51. Suzuki, S., Shiraishi, M., Shibayama, H. & Asada, M. High-power operation of terahertz oscillators with resonant tunneling diodes using impedance-matched antennas and array configuration. *IEEE J. Sel. Top. Quantum Electron.* **19**, 8500108 (2013).
52. Duffy, S. M. et al. Accurate modeling of dual dipole and slot elements used with photomixers for coherent terahertz output power. *IEEE Trans. Microw. Theory Tech.* **49**, 1032–1038 (2001).
53. Ito, H., Nakajima, F., Furuta, T. & Ishibashi, T. Continuous THz-wave generation using antenna-integrated unitravelling-carrier photodiodes. *Semicond. Sci. Technol.* **20**, S191S198 (2005).
54. Yang, S. & Jarrahi, M. High-power continuous-wave terahertz generation through plasmonic photomixers. *IEEE Int. Microw. Symp*. 1–4 (IEEE, 2016).
55. Yang, S.-H. et al. Tunable terahertz wave generation through a bimodal laser diode and plasmonic photomixer. *Opt. Express* **23**, 31206–31215 (2015).
56. Scheller, M., Yarborough, J. M., Moloney, J. V., Fallahi, M., Koch, M. & Koch, S. W. Room temperature continuous wave milliwatt terahertz source. *Opt. Express* **18**, 27112–27117 (2010).
57. Lu, Q., Wu, D., Sengupta, S., Slivken, S. & Razeghi, M. Room temperature continuous wave, monolithic tunable THz sources based on highly efficient mid-infrared quantum cascade lasers. *Sci. Rep.* **6**, 23595 (2016).
58. Hayashi, S. et al. High-brightness continuously tunable narrowband subterahertz wave generation.*IEEE Trans. Terahertz Sci. Tech.* **6**, 858–861 (2016).
59. Huang, D. et al. 324 GHz CMOS frequency generator using linear superposition technique. *Dig. Tech. Pap. IEEE Int. Solid State Circuits Conf.* 476–477 (2008).
60. Seok, E. et al. A 410 GHz CMOS push–push oscillator with an on-chip patch antenna. *Dig. Tech. Pap. IEEE Int. Solid State Circuits Conf.* 472–473 (2008).
61. Hu, Z., Kaynak, M. & Han, R. High-power radiation at 1 THz in silicon: a fully scalable array using a multi-functional radiating mesh structure. *IEEE J. Solid State Circuits* **53**, 1313–1327 (2018).
62. Ahmad, Z., Lee, M. & K. K. O. 1.4 THz, −13 dBm-EIRP frequency multiplier chain using symmetric- and asymmetric-CV varactors in 65 nm CMOS. *Dig. Tech. Pap. IEEE Int. Solid State Circuits Conf.* 350–351 (2016).
63. Han, R. et al. A SiGe terahertz heterodyne imaging transmitter with 3.3 mW radiated power and fully-integrated phase-locked loop. *IEEE J. Solid State Circuits*, **50**, 2935–2947 (2015).
64. Pfeiffer, U. R. et al. A 0.53 THz reconfigurable source array with up to 1 mW radiated power for terahertz imaging applications in 0.13 µm SiGe BiCMOS. *Dig. Tech. Pap. IEEE Int. Solid State Circuits Conf.* 256–257 (2014).
65. Gonzalez, G. *Microwave Transistor Amplifiers: Analysis and Design*. 2nd edn, (Prentice-Hall, Upper Saddle River, 1997).
66. Mei, X. et al. First demonstration of amplification at 1 THz using 25-nm InP high electron mobility transistor process. *IEEE Electron Dev. Lett.* **36**, 327–329 (2015).
67. Urteaga, M. et al. 130 nm InP DHBTs with f_t> 0.52 THz and fmax>1.1 THz. In *Proc. 69th Annu. Device Res. Conf.* 281–282 (IEEE, 2011).
68. Alexandrova, M., Flüeckiger, R., Lövblom, R., Ostinelli, O. & Bolognesi, C. R. GaAsSb-based DHBTs with a reduced base access distance and f_T/f_{MAX} = 503/780 GHz. *IEEE Electron Dev. Lett.* **35**, 1218–1220 (2014).
69. Bolognesi, C. R. et al. InP/GaAsSb DHBTs for THz applications and improved extraction of their cutoff frequencies. *IEEE Int. Electron Dev. Meeting Tech. Dig.* 723–726 (2016).
70. Shinohara, K. et al. Scaling of GaN HEMTs and Schottky diodes for submillimeter-wave MMIC applications. *IEEE Trans. Electron Dev.* **60**, 2982–2996 (2013).
71. Planes, N. et al. 28 nm FDSOI technology platform for high-speed low-voltage digital applications. *Proc. Symp. VLSI Technol.* 133–134 (2012).
72. Pekarik, J. J. et al. A 90nm SiGe BiCMOS technology for mm-wave and high performance analog applications. In *Proc. Bipolar/BiCMOS Circuits and Technology Meeting* 92–95 (IEEE, 2014).
73. Huylenbroeck, S. V. et al. Pedestal collector optimization for high speed SiGe:C HBT. In *Proc. Bipolar/BiCMOS Circuits and Technology Meeting* 66–69 (IEEE, 2011).
74. Heinemann, B. et al. SiGe HBT technology with f_T/f_{max} of 300GHz/500GHz and 2.0 ps CML gate delay. In *IEEE Int. Electron Devices Meeting* 30.5.1–30.5.4 (IEEE, 2010).

75. Heinemann, B. et al. SiGe HBT with f_T/f_{max} of 505 GHz/720 GHz. *IEEE Int. Electron Devices Meeting* 51–54 (IEEE, 2016).
76. Sengupta, K. & Hajimiri, A. 0.28 THz power-generation and beam-steering array in CMOS based on distributed active radiators. *IEEE J. Solid State Circuits* **47**, 3013–3031 (2012).
77. Jiang, C. et al. A fully integrated 320 GHz coherent imaging transceiver in 130 nm SiGe BiCMOS. *IEEE J. Solid State Circuits*, **51**, 2596–2609 (2016).
78. Al Hadi, R. et al. A 1 k-pixel video camera for 0.7–1.1 terahertz imaging applications in 65-nm CMOS. *IEEE J. Solid State Circuits,* **47**, 2999–3012 (2012).
79. Park. J., Kang, S., Thyagarajan, S., Alon, E. & Niknejad, A. M. A 260 GHz fully integrated CMOS transceiver for wireless chip-to-chip communication. *2012 Symp. VLSI Circuits* 48–49 (IEEE, 2012).
80. Katayama, K. et al. A 300 GHz CMOS transmitter with 32-QAM 17.5 Gb/s/ch capability over six channels. *IEEE J. Solid State Circuits* **51**, 3037–3048 (2016).
81. Momeni, O. & Afshari, E. High power terahertz and millimeter-wave oscillator design: a systematic approach. *IEEE J. Solid State Circuits* **46**, 583–597 (2011).
82. Steyaert, W. & Reynaert, P. A 0.54 THz signal generator in 40 nm bulk CMOS with 22 GHz tuning range and integrated planar antenna. *IEEE J. Solid State Circuits* **49**, 1617–1626 (2014).
83. Zhao, Y. et al. A 0.56 THz phase-locked frequency synthesizer in 65 nm CMOS technology. *IEEE J. Solid State Circuits* **51**, 3005–3019 (2016).
84. Öjefors, E. et al. A 820 GHz SiGe chipset for terahertz active imaging applications. *Dig. Tech. Pap. IEEE Int. Solid State Circuits Conf.* 224–225 (2011).
85. Aghasi, H., Cathelin, A. & Afshari, E. A 0.92-THz SiGe power radiator based on a nonlinear theory for harmonic generation. *IEEE J. Solid State Circuits* **52**, 406–422 (2017).
86. Tousi, Y. & Afshari, E. A High-power and scalable 2-D phased array for terahertz CMOS integrated system. *IEEE J. Solid State Circuits* **50**, 597–609 (2015).
87. Jameson, S., Halpern, E. & Socher, E. A 300 GHz wirelessly locked 2×3 array radiating 5.4dBm with 5.1% DC-to-RF efficiency in 65nm CMOS. *Dig. Tech. Pap. IEEE Int. Solid State Circuits Conf.* 348–349 (2016).
88. Zhao, Y. et al. A 0.54–0.55 THz 2×4 coherent source array with EIRP of 24.4 dBm in 65nm CMOS technology. *IEEE MTT-S Int. Microw. Symp.* 1–3 (2015).
89. Assefzadeh, M. M. & Babakhani, A. broadband oscillator-free THz pulse generation and radiation based on direct digital-to-impulse architecture. *IEEE J. Solid State Circuits* **52**, 2905–2919 (2017).
90. Wu, X. & Sengupta, K. Dynamic waveform shaping with picosecond time widths. *IEEE J. Solid State Circuits* **52**, 389–405 (2017).
91. Fang, T. et al. Detection of 3.0 THz wave with a detector in 65 nm standard CMOS process. In *IEEE Asian Solid State Circuits Conf.* 189–192 (IEEE, 2017).
92. Ahmad, Z., Lisauskas, A., Roskos, H. G. & K. K. O. 9.74-THz electronic far-infrared detection using Schottky barrier diodes in CMOS. *IEEE Int. Electron Devices Meeting* 4.4.1–4.4.4 (IEEE, 2014).
93. Dyakonov, M. & Shur, M. Shallow water analogy for a ballistic field effect transistor: new mechanism of plasma wave generation by DC current. *Phys. Rev. Lett.* **71**, 2465–2468 (1993).
94. Dyakonov, M. & Shur, M. Detection, mixing, and frequency multiplication of terahertz radiation by two-dimensional electronic fluid. *IEEE Trans. Electron Devices* **43**, 380–387 (1996).
95. Knap., W. et al. Nonresonant detection of terahertz radiation in field effect transistors. *J. Appl. Phys.* **91**, 9346–9353 (2002).
96. Shchepetov, A. et al. Oblique modes effect on terahertz plasma wave resonant detection in InGaAs/ InAlAs multichannel transistors. *Appl. Phys. Lett.* **92**, 242105 (2008).
97. Öjefors, E., Pfeiffer, U. R., Lisauskas, A. & Roskos, H. G. A 0.65 THz Focal-Plane Array in a Quarter-Micron CMOS Process Technology. *IEEE J. Solid State Circuits* **44**, 1968–1976 (2009).
98. Statnikov, K., Grzyb, J., Heinemann, B. & Pfeiffer, U. R. 160-GHz to 1-THz multi-color active imaging with a lens-coupled SiGe HBT chip-set. *IEEE Trans. Microw. Theory Tech.* **63**, 520–532 (2015).
99. Tang, A. & Chang, M. C. F. Inter-modulated regenerative CMOS receivers operating at 349 and 495 GHz for THz imaging applications. *IEEE Trans. Terahertz Sci. Technol.* **3**, 134–140 (2013).
100. Han, R. et al. Active terahertz imaging using Schottky diodes in CMOS: array and 860-GHz pixel. *IEEE J. Solid State Circuits* **48**, 2296–2308 (2013).
101. Sengupta, K., Seo, D. J., Yang, L. & Hajimiri, A. silicon integrated 280 GHz imaging chipset with 4× 4 SiGe receiver array and CMOS source. *IEEE Trans. Terahertz Sci. Tech.* **5**, 427–437 (2015).
102. Wu, X. & Sengupta, K. On-chip THz spectroscope exploiting electromagnetic scattering with multi-port antenna. *IEEE J. Solid State Circuits* **51**, 3049–3062 (2016).
103. Wu, X. & Sengupta, K. Single-chip source-free terahertz spectroscope across 0.04–0.99 THz: combining sub-wavelength near-field sensing and regression analysis. *Opt. Express* **26**, 7163–7175 (2018).
104. Hillger, P. et al. A 128-pixel 0.56 THz sensing array for real-time near-field imaging in 0.13 µm SiGe BiCMOS. *Dig. Tech. Pap. IEEE Int. Solid State Circuits Conf.* 418–419 (2018).
105. Thyagarajan, S. V., Kang, S. & Niknejad, A. M. A 240 GHz fully integrated wideband QPSK receiver in 65 nm CMOS. *IEEE J. Solid State Circuits* **50**, 2268–2280 (2015).
106. Sarmah, N. et al. A fully integrated 240-GHz direct-conversion quadrature transmitter and receiver chipset in SiGe technology. *IEEE Trans. Microw. Theory Tech.* **64**, 562–574 (2016).
107. Mendis, R. & Grischkowsky, D. Undistorted guided-wave propagation of subpicosecond terahertz pulses. *Opt. Lett.* **26**, 846–848 (2001).
108. Hermelo, M. F., Shih, P.-T., Steeg, M., Ng'oma, A. & Stöhr, A. Spectral efficient 64-QAM-OFDM terahertz communication link. *Opt. Express* **25**, 19360–19370 (2017).
109. Reichel, K., Mendis, R. & Mittleman, D. M. A broadband terahertz waveguide T-junction variable power splitter. *Sci. Rep.* **6**, 28925 (2016).
110. Karl, N. J., McKinney, R. W., Monnai, Y., Mendis, R. & Mittleman, D. M. Frequency-division multiplexing in the terahertz range using a leaky-wave antenna. *Nat. Photon.* **9**, 717–720 (2015).
111. Weidenbach, M. et al. 3D printed dielectric rectangular waveguides, splitters and couplers for 120 GHz. *Opt. Express* **24**, 28968–28976 (2016).
112. Yata, M., Fujita, M. & Nagatsuma, T. Photonic-crystal diplexers for terahertz-wave applications *Opt. Express* **24**, 7835–7849 (2016).
113. Ma, J., Weidenbach, M., Guo, R., Koch, M. & Mittleman, D. M. Communications with THz waves: switching data between two waveguides. *J. Infrared Millim. Terahertz Waves* **38**, 1316–1320 (2017).
114. Mottaghizadeh, A. et al. Nanoscale electromagnetic confinement in THz circuit resonators. *Opt. Express* **25**, 28718–28730 (2017).
115. Paulillo, B. et al. Circuit-tunable sub-wavelength THz resonators: hybridizing optical cavities and loop antennas. *Opt. Express* **22**, 21302–21312 (2014).
116. Zhang, Q. et al. Collective non-perturbative coupling of 2D electrons with high-quality-factor terahertz cavity photons. *Nat. Phys.* **12**, 1005–1011 (2016).
117. Mendis, R. & Mittleman, D. M. Artificial dielectrics: ordinary metallic waveguides mimic extraordinary dielectric media. *IEEE Microw. Mag.* **15**, 34–42 (2014).
118. Mendis, R., Nag, A., Chen, F. & Mittleman, D. M. A tunable universal terahertz filter using artificial dielectrics based on parallel-plate waveguides. *Appl. Phys. Lett.* **97**, 131106 (2010).
119. Mendis, R., Nagai, M., Zhang, W. & Mittleman, D. M. Artificial dielectric polarizing-beamsplitter and isolator for the terahertz region. *Sci. Rep.* **7**, 5909 (2017).
120. Reichel, K.S. et al. Electrically reconfigurable terahertz signal processing devices using liquid metal components. *Nat. Commun.* **9**, 4202 (2018).
121. Han, Z., Kohno, K., Fujita, H., Hirakawa, K. & Toshiyoshi, H. Tunable terahertz filter and modulator based on electrostatic MEMS reconfigurable SRR array. *IEEE J. Sel. Top. Quantum Electron.* **21**, 2700809 (2014).
122. Sensale-Rodriguez, B., Yan, R., Liu, L., Jena, D. & Xing, H. G. Graphene for reconfigurable terahertz optoelectronics. *Proc. IEEE* **101**, 1705–1716 (2013).
123. Chen, H.-T. et al. Active terahertz metamaterial devices. *Nature* **444**, 597–600 (2006).
124. Mittendorff, M., Li, S. & Murphy, T. E. Graphene-based waveguide-integrated terahertz modulator. *ACS Photon.* **4**, 316–321 (2017).
125. Karl, N. et al. An electrically driven terahertz metamaterial diffractive modulator with more than 20 dB of dynamic range. *Appl. Phys. Lett.* **104**, 091115 (2014).
126. Zhang, Y. et al. Gbps terahertz external modulator based on a composite metamaterial with a double-channel heterostructure. *Nano Lett.* **15**, 3501–3506 (2015).
127. Singh, P. K. & Sonkusale, S. High speed terahertz modulator on the chip based on tunable terahertz slot waveguide. *Sci. Rep.* **7**, 40933 (2017).
128. Sengupta, K. & Hajimiri, A. Designing optimal surface currents for efficient on-chip mm-wave radiators with active circuitry. *IEEE Trans. Microw. Theory Tech.* **64**, 1976–1988 (2016).
129. Monnai, Y. et al. Terahertz beam steering and variable focusing using programmable diffraction gratings. *Opt. Express* **21**, 2347–2354 (2013).
130. Scherger, B. et al. Discrete terahertz beam steering with an electrically controlled liquid crystal device. *J. Infrared Millim. Terahertz Waves* **33**, 1117–1122 (2012).
131. Jha, K. R. & Singh, G. Terahertz planar antennas for future wireless communication: a technical review. *Infrared Phys. Technol.* **60**, 71–80 (2013).
132. Xu, Z., Dong, X. & Bornemann, J. Design of a reconfigurable MIMO system for THz communications based on graphene antennas. *IEEE Trans. Terahertz Sci. Technol.* **4**, 609–617 (2014).

133. Akyildiz, I. F. & Jornet, J. M. Realizing ultra-massive mimo (1024×1024) communication in the (0.06–10) terahertz band. *Nano Commun. Netw.* **8**, 46–54 (2016).
134. Ma, J., Karl, N. J., Bretin, S., Ducournau, G. & Mittleman, D. M. Frequency-division multiplexer and demultiplexer for terahertz wireless links. *Nat. Commun.* **8**, 729 (2017).
135. Ma, J., Shrestha, R., Moeller, L. & Mittleman, D. M. Channel performance of indoor and outdoor terahertz wireless links. *APL Photon.* **3**, 051601 (2018).
136. Koenig, S. et al. Wireless sub-THz communication system with high data rate. *Nat. Photon.* **7**, 977–981 (2013).
137. Nagatsuma, T., Ducournau, G. & Renaud, C. C. Advances in terahertz communications accelerated by photonics. *Nat. Photon.* **10**, 371–379 (2016).
138. Nagatsuma, T. & Carpintero, G. Recent progress and future prospect of photonics-enabled terahertz communications research. *IEICE Trans. Electron.* **E98C**, 1060–1070 (2015).
139. Nagatsuma, T. et al. Real-time 100-Gbit/s QPSK transmission using photonics-based 300-GHz-band wireless link. In *2016 IEEE Int. Topical Meet. Microw. Photon.* 27–30 (IEEE, 2016).
140. Jia, S. et al. 0.4 THz photonic-wireless link with 106 Gb/s single channel bitrate. *J. Lightwave Technol.* **36**, 610–616 (2018).
141. Pang, X. et al. 260 Gbit/s photonic–wireless link in the THz band. In *Proc. 2016 IEEE Photon. Conf.* 1–2 (IEEE, 2016).
142. Hulme, J. et al. Fully integrated microwave frequency synthesizer on heterogeneous silicon- III/V. *Opt. Express* **25**, 2422–2431 (2017).
143. Carpintero, G. et al. Microwave photonic integrated circuits for millimeter-wave wireless communications. *J. Lightwave Technol.* **32**, 3495–3501 (2014).
144. Balakier, K., Ponnampalam, L., Fice, M. J., Renaud, C. C. & Seeds, A. J. Integrated semiconductor laser optical phase lock loops. *IEEE J. Sel. Top. Quantum Electron.* **24**, 1500112 (2018).
145. Carpintero, G. et al. Wireless data transmission at terahertz carrier waves generated from a hybrid InP-polymer dual tunable DBR laser photonic integrated circuit. *Sci. Rep.* **8**, 3018 (2018).
146. Volkaerts, W., Van Thienen, N. & Reynaert, P. An FSK plastic waveguide communication link in 40 nm CMOS. *Dig. Tech. Pap. IEEE Int. Solid State Circuits Conf.* 178–179 (2015).
147. Van Thienen, N., Zhang, Y., De Wit., M. & Reynaert, P. An 18 Gbps polymer microwave fiber (PMF) communication link in 40 nm CMOS. In *IEEE European Solid State Circuits Conf.* 483–486 (IEEE, 2016).
148. Fischer, B., Hoffmann, M., Helm, H., Modjesch, G. & Jepsen, P. U. Chemical recognition in terahertz time-domain spectroscopy and imaging. *Semicond. Sci. Technol.* **20**, S246–S253 (2005).
149. Kawase, K., Ogawa, Y., Watanabe, Y. & Inoue, H. Non-destructive terahertz imaging of illicit drugs using spectral fingerprints. *Opt. Express* **11**, 2549–2554 (2003).
150. Mittleman, D. M., Jacobsen, R. H., Neelamani, R., Baraniuk, R. G. & Nuss, M. C. Gas sensing using terahertz time-domain spectroscopy. *Appl. Phys. B* **67**, 379–390 (1998).
151. Sampaolo, A. et al. Improved tuning fork for terahertz quartz-enhanced photoacoustic spectroscopy. *Sensors* **16**, 439 (2016).
152. Wang, C., Perkins, B., Wang, Z. & Han, R. Molecular detection for unconcentrated gas with ppm sensitivity using 220-to-320-GHz dual-frequency-comb spectrometer in CMOS. *IEEE Trans. Biomed. Circuits Syst.* **12**, 709–721 (2018).
153. Watts, C. M. et al. Terahertz compressive imaging with metamaterial spatial light modulators. *Nat. Photon.* **8**, 605–609 (2014).
154. Hunt, J. et al. Metamaterial apertures for computational imaging. *Science* **339**, 310–313 (2013).
155. IEEE standard for high data rate wireless multi-media networks–amendment 2, 100 Gb/s wireless switched point-to-point physical layer. In *IEEE Std 802.15.3d-2017 (amendment to IEEE Std 802.15.3–2016 as amended by IEEE Std 802.15.3e-2017)* 1–55 (IEEE, 2017).
156. Shahramian, S., Holyoak, M., Singh, S., Farahani, B. J. & Baeyens, Y. A fully integrated scalable W-band phased-array module with integrated antennas, self-alignment and self-test. *Dig. Tech. Pap. IEEE Int. Solid State Circuits Conf.* 74–76 (2018).
157. Nagatsuma, T., Oogimoto, K., Inubushi, Y. & Hirokawa, J. Practical considerations of terahertz communications for short distance applications. *Nano Commun. Netw.* **10**, 1–12 (2016).
158. Petrov, V. et al. Last meter indoor terahertz wireless access: performance insights and implementation roadmap. *IEEE Commun. Mag.* **56**, 158–165 (2018).
159. Elayan, H., Amin, O., Shubair, R. M. & Alouini, M. Terahertz communication: the opportunities of wireless technology beyond 5G. In *Int. Conf. Advanced Communication Technologies and Networking* 1–5 (IEEE, 2018).
160. Rappaport, T. et al. Millimeter wave mobile communications for 5G cellular: it will work! *IEEE Access* **1**, 335–349 (2013).

Acknowledgements

The authors acknowledge the National Science Foundation, Office of Naval Research, the Army Research Office, the W. M. Keck Foundation, the Ministry of Internal Affairs and Communications (MIC) Japan and the Japan Science and Technology Agency (JST) for funding and all the group members of technical inputs.

Author contributions

All of the authors contributed to writing the manuscript.

Competing interests

The authors declare no competing interests.

Additional information

Reprints and permissions information is available at www.nature.com/reprints.

Correspondence should be addressed to K.S.

Publisher's note: Springer Nature remains neutral with regard to jurisdictional claims in published maps and institutional affiliations.